Perturbative Quantum Simulation

Jinzhao Sun, Suguru Endo, Huiping Lin, Patrick Hayden, Vlatko Vedral, and Xiao Yuan

Phys. Rev. Lett. **129**, 120505 — Published 15 September 2022

DOI: 10.1103/PhysRevLett.129.120505

Perturbative quantum simulation

Jinzhao Sun,[1,2,3] Suguru Endo,[4] Huiping Lin,[1,5] Patrick Hayden,[6] Vlatko Vedral,[2,7] and Xiao Yuan[1,5,6,*]

[1] *Center on Frontiers of Computing Studies, Peking University, Beijing 100871, China*
[2] *Clarendon Laboratory, University of Oxford, Parks Road, Oxford OX1 3PU, United Kingdom*
[3] *Quantum Advantage Research, Beijing 100080, China*
[4] *NTT Computer & Data Science Laboratories, NTT corporation, Musashino, Tokyo 180-8585, Japan*
[5] *School of Computer Science, Peking University, Beijing 100871, China*
[6] *Stanford Institute for Theoretical Physics, Stanford University, Stanford California 94305, USA*
[7] *Centre for Quantum Technologies, National University of Singapore, Singapore 117543,Singapore*

(Dated: August 22, 2022)

Approximation based on perturbation theory is the foundation for most of the quantitative predictions of quantum mechanics, whether in quantum many-body physics, chemistry, quantum field theory or other domains. Quantum computing provides an alternative to the perturbation paradigm, yet state-of-the-art quantum processors with tens of noisy qubits are of limited practical utility. Here, we introduce perturbative quantum simulation, which combines the complementary strengths of the two approaches, enabling the solution of large practical quantum problems using limited noisy intermediate-scale quantum hardware. The use of a quantum processor eliminates the need to identify a solvable unperturbed Hamiltonian, while the introduction of perturbative coupling permits the quantum processor to simulate systems larger than the available number of physical qubits. We present an explicit perturbative expansion that mimics the Dyson series expansion and involves only local unitary operations, and show its optimality over other expansions under certain conditions. We numerically benchmark the method for interacting bosons, fermions, and quantum spins in different topologies, and study different physical phenomena, such as information propagation, charge-spin separation, and magnetism, on systems of up to 48 qubits only using an $8+1$ qubit quantum hardware. We experimentally demonstrate our scheme on the IBM quantum cloud, verifying its noise robustness and illustrating its potential for benchmarking large quantum processors with smaller ones.

A universal quantum computer can naturally simulate the real-time dynamics of any closed finite dimensional quantum system [1], a challenging task for classical computers. While there has been tremendous progress in quantum computing hardware development, including the landmark quantum supremacy/advantage experiments with superconducting and optical systems [2–5], state-of-the-art quantum hardware can still only control tens of noisy qubits [2, 5–7]. That is insufficient for the implementation of fault-tolerant universal quantum computing, which requires 10^3 or more physical qubits per logical qubit to suppress the physical error [8]. It is more pragmatic in the near term to focus on the noisy intermediate-scale quantum (NISQ) regime and utilise hybrid methods, which run a shallow circuit without implementing full error correction [9]. Nevertheless, most quantum simulation algorithms, whether targeting NISQ or universal quantum computers, generally entails a number of physical or logical qubits no smaller than the problem size [10–12]. Given that large-scale fault-tolerant quantum computers do not yet exist and there will be significant size constraints even on NISQ devices for the foreseeable future, a pressing question is how to solve large practical problems with limited quantum devices [13, 14].

One possibility is to leverage the classical methods that have been developed to solve quantum many-body problems, wherein the most successful one is perturbation theory. This method divides the Hamiltonian into a major but easily solved component and a weak but potentially complicated counterpart, in which case the full dynamics can be expressed as a series expansion [15–20]. However, the ability to solve the major component and compute the higher-order expansions limits the use of perturbation theory in classical simulation of general many-body problems.

Here, we propose perturbative quantum simulation (PQS), which directly simulates the major component on a quantum computer while perturbatively approximate the weak interaction component. Since there is no assumption on the size or interaction of the major component, PQS potentially goes beyond the conventional perturbative approach, and it could simulate classically challenging systems, such as large systems with weak inter-subsystem interactions or intermediate systems with general interactions. Compared to universal quantum computing, PQS has limited power for arbitrary problems; yet, the perturbative treatment of the weak component greatly reduces quantum resources compared with conventional quantum simulation. Notably, PQS runs a shallower circuit with fewer qubits, making it more noise-robust and thus useful in benchmarking large quantum devices with smaller ones. Our experiments on the IBM quantum devices demonstrate a significant improvement of the simulation accuracy over direct simulation.

For eigenstate problems, there are considerable hybrid schemes that combines different classical methods, such as density matrix embedding theory [21–24], dynamical

mean field theory [25–27], density functional theory embedding [28], quantum defect embedding theory [29, 30], tensor networks [31, 32], entanglement forging [33, 34], virtual orbital approximation [35], quantum Monte Carlo [36–41], etc. Our work instead focuses on the different but meaningful dynamics problem, which is based on perturbation theory and fundamentally from existing ones with different assumptions, limitations, or applications [42].

Background.—We consider to simulate the dynamics of a quantum many-body system. Suppose the whole system is divided into L subsystems according to topological structures or degrees of freedom, like the clustered molecules [43], the Hamiltonian is $H = H^{\text{loc}} + V^{\text{int}}$, where $H^{\text{loc}} = \sum_l H_l$ is the local strong interaction with each H_l acting on the lth subsystem, and $V^{\text{int}} = \sum_j \lambda_j V_j^{\text{int}}$ is the weak perturbative interaction between the subsystems. Here V_j^{int} are different types of interactions with real amplitudes λ_j.

To simulate the dynamics of $U(t) = e^{-iHt}$, a representative perturbation treatment is via Dyson series expansion as

$$U(t) = 1 - i\int_{t_0}^{t} dt_1 e^{iH^{\text{loc}}(t_1-t_0)} V^{\text{int}} e^{-iH^{\text{loc}}(t_1-t_0)} + \dots \tag{1}$$

Then $U(t)$ becomes a linear combination of trajectories consisting of different sequential unitary operators. When the local Hamiltonians $\{H_l\}$ are solvable, one can further represent the expansion graphically, such as via Feynman diagrams, and compute expectation values of the time evolved state with different graphs corresponding to different expansion terms. A major limitation of perturbation theory is the assumption of the simple hence solvable local Hamiltonians, which fails when $\{H_l\}$ become strongly correlated, as that happens in realistic systems. Indeed, even if no interaction under certain partitioning strategy with $V^{\text{int}} = 0$, no classical methods exist that can efficiently simulate the dynamics of general Hamiltonian $H^{\text{loc}} = \sum_l H_l$, otherwise the computational class of bounded-error quantum polynomial time collapses. In the following, we introduce the framework of PQS, based on which we propose an explicit algorithm mimicking Dyson series expansion and show its optimality over more general theories.

Framework.—Here, we focus on general ways that realise the joint time evolution channel $\mathcal{U}(\rho, T) = U(T)\rho U^\dagger(T)$ by applying only local operations on each subsystem separately. To do so, we first introduce the concept of local *generalised quantum operations*

$$\Phi(\rho) = \text{Tr}_E\left[\mathbf{U}\left(\rho \otimes |\mathbf{0}\rangle\langle\mathbf{0}|_E\right)\mathbf{V}^\dagger\right]. \tag{2}$$

Here we denote ancillary states $|\mathbf{0}\rangle\langle\mathbf{0}|_E = |0\rangle\langle 0|_{E_1} \otimes \cdots \otimes |0\rangle\langle 0|_{E_L}$ and unitary operators $\mathbf{U} = U_{1E_1} \otimes \cdots \otimes U_{LE_L}$ and $\mathbf{V} = V_{1E_1} \otimes \cdots \otimes V_{LE_L}$, where U_{jE_j} and V_{jE_j} represents the operators acting only on the subsystem j and the jth ancilla. While the operation $\Phi(\rho)$ is nonphysical in general, it can be realised effectively using local operations and postprocessing (see [44]). Note that $\Phi(\rho)$ reduces to local quantum channels when $\mathbf{U} = \mathbf{V}$. The key idea of PQS theories is to decompose the joint evolution into a set of generalised quantum operations, which separately act on each subsystem. By choosing a spanning set of $\{\Phi_k\}$ properly, an infinitesimal evolution governed by the interaction $\mathcal{V}(\delta t)[\rho] = V^{\text{int}}(\delta t)\rho V^{\text{int}}(\delta t)^\dagger$ can be decomposed as

$$\mathcal{V}(\delta t)[\rho] = \mathcal{I}(\rho) + \delta t \sum_k \alpha_k \Phi_k(\rho) \tag{3}$$

where $V^{\text{int}}(\delta t) = e^{-iV^{\text{int}}\delta t}$ represents the interacting unitary operations within duration δt, and $\mathcal{I}$ is the identity operation.

Next, we consider a Trotterised joint evolution as $\mathcal{U}(T) = [\mathcal{V}(\delta t) \circ \bigotimes_l \mathcal{U}_l(\delta t)]^{T/\delta t}$. Using the decomposition in Eq. (3), we can then expand $\mathcal{U}(T)$ as a series of different trajectories. Here, each trajectory is defined by which operations act at each time, including the local time evolution $\mathcal{U}_l(\delta t)$ of each subsystem and one of the generalised quantum operation $\Phi_k(\rho)$ that on average emulates the nonlocal effect of $\mathcal{V}^{\text{int}}$. The whole evolution $\mathcal{U}(T)$ is now decomposed as a linear combination of local operations that act separately on each subsystem, which can be effectively realised in parallel. The expectation value of an arbitrary state can be obtained from local measurement results (see Sec. IB in [44] for the derivation and implementation).

The above discretised scheme assumes a small discrete timestep and requires to apply the operations at each time step δt, which is unnecessary since the effect of the weak interacting operation $\mathcal{V}(\delta t)$ in a short time is close to the identity. We address this problem by stochastically applying the operation Φ_k depending on the amplitude of its associated coefficient $|\alpha_k|$. Taking a short time limit $\delta t \to 0$, we generate each trajectory according to the decomposition in Eq. (3) and stochastically realise the joint time evolution with operations separately acting on each subsystem. The average of different trajectories reproduces the joint dynamics under $\mathcal{U}(T)$. Note that the number of generalised quantum operations required to realise the joint evolution scales proportionally to the interaction strength as $\mathcal{O}(\sum_k |\alpha_k| T)$, and on average the stochastic implementation scheme is proven to be equivalent to the discretised scheme (See Sec. IC in [44]).

By applying our algorithm, the whole simulation process is now decomposed into the average of different ones, each of which only involves operations on the subsystems. Thus, we can effectively simulate nL qubits with operations on subsystems with only $\mathcal{O}(n)$ qubits,

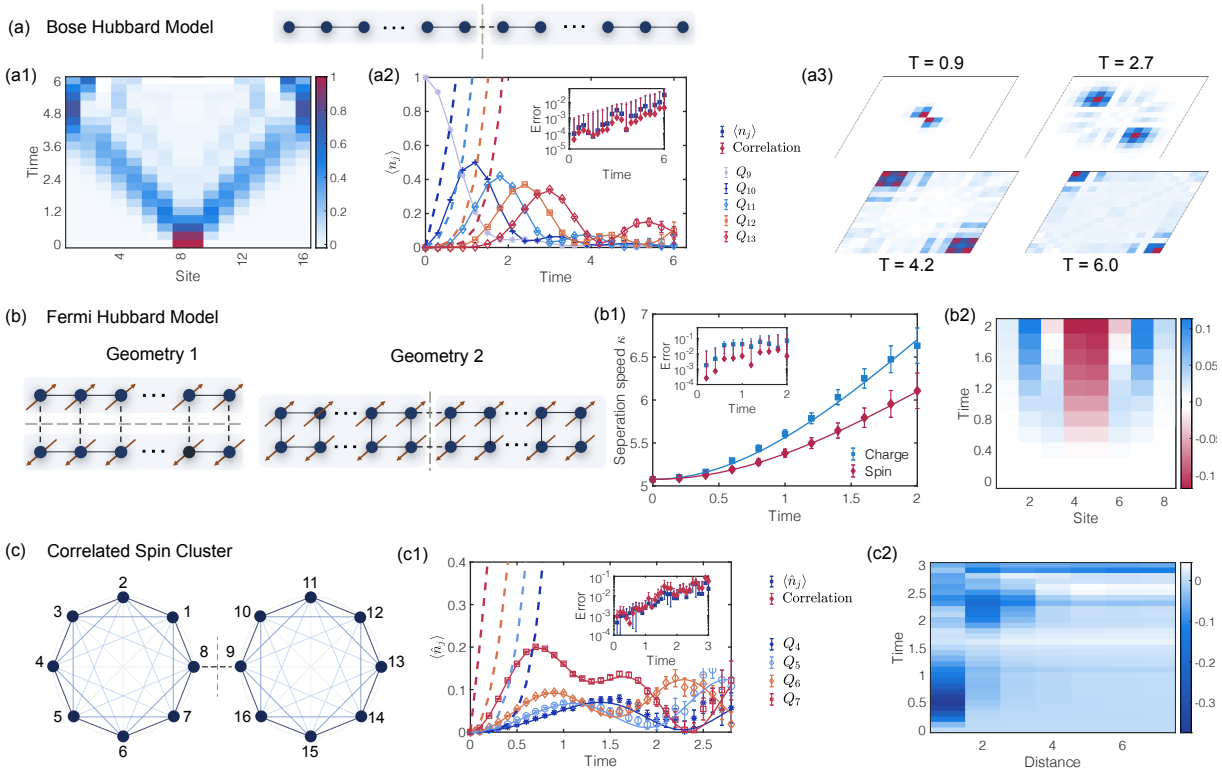

FIG. 1. Dynamics simulation of interacting (a) bosons, (b) fermions, and (c) quantum spin systems with different topologies. Gray dashed lines in site-edge diagrams manifest subsystem partitioning for PQS. We group 8 qubits as a subsystem to simulate $N = 16$-qubit quantum systems using most 5×10^5 samples. Solid lines represent exact results from direct simulation. (a) Quantum walk (QW) of spinless bosons on a 1D array in the large onsite repulsion limit (see Sec. VI in [44] for the Hamiltonian). Two identical bosons are initially excited at the centre. (a1) Density spreading $\langle \hat{n}_j \rangle = \langle \hat{b}_j^\dagger \hat{b}_j \rangle$ with bosonic operators $\hat{b}$ under time evolution. (a2) The density distribution at site 9 - 13 (labelling from left to right). The nearest-neighbour Lieb-Robinson bounds (dashed) capture the density spreading [6, 45, 46]. The inset shows the errors for the average density and the average density-density correlator $\hat{\rho}_{ij} = \langle \hat{b}_i^\dagger \hat{b}_j^\dagger \hat{b}_i \hat{b}_j \rangle$ with respect to the exact results. (a3) Boson spatial antibunching in QW. The normalised correlator $\hat{\rho}_{ij}/\hat{\rho}_{ij}^{\max}$ at different t [47, 48]. (b) Separation of charge and spin density (CSD) in a 1D Fermi-Hubbard model $H = -J\sum_{j,\sigma}\left(\hat{c}_{j,\sigma}^\dagger \hat{c}_{j+1,\sigma} + \text{h.c.}\right) + U\sum_j \hat{n}_{j,\uparrow}\hat{n}_{j,\downarrow} + \sum_{j,\sigma} h_{j,\sigma}\hat{n}_{j,\sigma}$ ($\hat{c}_{j,\sigma}$, $\hat{c}_{j,\sigma}^\dagger$: fermionic operators with spin σ, $U = J = 0.5$) [48]. Left: two partitioning strategies for small and large on-site potential U. The initial state is the ground state of a non-interacting Hamiltonian with quarter filling ($N_\uparrow = N_\downarrow = 2$), in which the CSD are generated in the middle of the chain at $t = 0$ [49–51]. (b1) The separation of charge (blue square) and spin (red diamond) densities. We characterise the separation speed from the middle as $\kappa_\pm = \sum_{j=1}^N |j - (N+1)/2|\left(\langle \hat{n}_{j,\uparrow}\rangle \pm \langle \hat{n}_{j,\downarrow}\rangle\right)$ for charge (+) and spin (−) degrees of freedom with $\langle \hat{n}_j \rangle = \langle \hat{c}_j^\dagger \hat{c}_j \rangle$ ($N = 8$). The inset shows the errors under evolution. (b2) The difference of CSD under evolution. The relative separation is initially set as 0. (c) Information propagation of correlated Ising spin clusters with power law decay interactions $H_l^{\text{loc}} = \sum_{ij} J_{ij}\hat{\sigma}_{l,i}^x \hat{\sigma}_{l,j}^x + h\sum_j \hat{\sigma}_{l,j}^z$ ($J_{ij} = |i-j|^{-1}$) in the subsystems and interaction $V^{\text{int}} = \hat{\sigma}_{1,N}^x \hat{\sigma}_{2,1}^x$ on the boundary. The initial state is prepared as $|\psi_0\rangle = \hat{\sigma}_8^x |0\rangle^{\otimes N}$. (c1) The signal of quasiparticle excitations at different sites, where the propagation is faster than the nearest-neighbour Lieb-Robinson velocity (dashed) [45, 52, 53]. (c2) The dynamics of the correlation function $C_d = \langle \hat{\sigma}_8^z \hat{\sigma}_{8+d}^z \rangle - \langle \hat{\sigma}_8^z \rangle \langle \hat{\sigma}_{8+d}^z \rangle$. The inset shows the errors for the averaged quasiparticle excitations density and correlation functions.

and this also offers noise robustness of our method (see Sec. VII in [44]). Note that local dynamics $\mathcal{U}_l(t)$ could be implemented with any Hamiltonian simulation methods, such as product formulae [54, 55] or quantum signal processing [56, 57], and our algorithm is compatible with both near-term and fault-tolerant quantum computers.

Explicit protocol.—While the decomposition of Eq. (3) holds in general for a (over)complete set of $\{\Phi_k\}$, it may involve difficult-to-implement operations in experiments. Here, we address this problem by developing an explicit decomposition with only local unitary operations. Specifically, we consider a natural expansion of $\mathcal{V}(\delta t)$ as

$$\mathcal{V}(\delta t)[\rho] = \mathcal{I}(\rho) - i\delta t \sum_j \lambda_j (V_j^{\text{int}}\rho - \rho V_j^{\text{int}}), \qquad (4)$$

where all V_j^{int} are tensor products of unitaries, and hence each term $\mathcal{I}(\rho)$, $V_j^{\text{int}}\rho$, or ρV_j^{int} corresponds to a specific

generalised quantum operation. We emphasise that the expansion only involves unitary operations, and avoids the computational cost in diagrammatic perturbation theory, which greatly simplifies the implementation. We further prove in Theorem 3 in [44] that the explicit decomposition corresponds to the infinite-order Dyson series expansion [58].

Implementing the interaction $\mathcal{V}$ perturbatively using generalised quantum operations introduces a sampling overhead C. Specifically, when measuring the output state of the perturbatively simulated state, the measurement accuracy is $\varepsilon = \mathcal{O}(C\sigma/\sqrt{N_s})$ given N_s samples in contrast to $\varepsilon = \mathcal{O}(1/\sqrt{N_s})$ in direct simulation. Here, σ is the standard deviation introduced from the expansion, normally less than 1. Assuming the general decomposition of Eq. (3), the overhead is $C = e^{\sum_k |\alpha_k| T}$. Different decomposition of Eq. (3) would lead to different coefficients and hence different overhead. We further prove that the explicit decomposition in Eq. (4) has the minimal simulation cost, provided that the Pauli operators of each V_i satisfy a certain mild condition (see Theorem 2 in [44] for the proof of optimality and illustrative examples here in [59]). Since the overhead increases exponentially with $\lambda_T = \sum_i |\lambda_i| T$, PQS cannot simulate arbitrary systems with strong V^{int} or long time T. Yet, the overhead is independent of the initial state, size and interaction strengths of the subsystems. With a constant λ_T, PQS can be applied to study intricate quantum many-body systems with strong subsystem interactions. As shown shortly, PQS can be used to probe interesting physical phenomena directly, benchmark NISQ processors, simulate large quantum circuits, etc.

Numerical and experimental results.—We apply PQS to study many-body physical phenomena in different systems with different topological structures. As shown in Fig. 1, we investigate (a) the quantum walk of bosons on a one-dimensional lattice, (b) the separation of charge and spin excitations of fermions with two-dimensional topology, and (c) the correlation propagation of quantum spin systems of two clusters. We design appropriate partitioning strategies, in which the whole system consists of two subsystems and each subsystem consists of 8 qubits. In each example, we present the corresponding task-specific partitioning strategy of the quantum systems. Using the explicit decomposition strategy, we exploit $8+1$ qubits to simulate each subsystem and classically emulate the quantum system with numerical results shown in Fig. 1. All unique features are detected just as we directly simulate the whole system. Indeed, the numerical results align with those of the exact simulation, thus verifying the reliability of the theory. We refer to Sec. VI in [44] for other physical systems, including the long-range spin chains, and simulation details.

These numerical tests are restricted to 16 qubits since

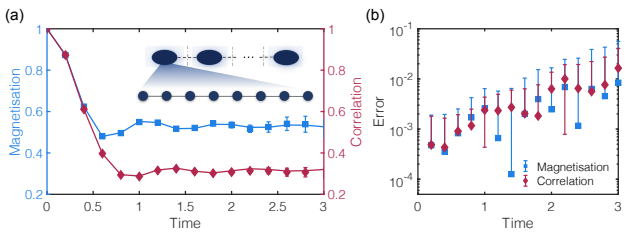

FIG. 2. Dynamics simulation of 1D 48-site spin chains. The subsystem and interaction Hamiltonians are $H_l^{\text{loc}} = \sum_i \hat{\sigma}_{l,i}^x \hat{\sigma}_{l,i+1}^x + \sum_i \hat{\sigma}_{l,i}^z$ and $V_l^{\text{int}} = f_l \hat{\sigma}_{l,N}^x \hat{\sigma}_{l+1,1}^x$, respectively, and the interactions on the boundary are randomly generated from $[0, J/2]$. (a) The average magnetisation (in blue) $\frac{1}{N}\sum_i \langle \hat{\sigma}_i^z \rangle$ and nearest-neighbour correlation function (in red) $\frac{1}{N-1}\sum_i \langle \hat{\sigma}_i^z \hat{\sigma}_{i+1}^z \rangle$, compared with TEBD method as a benchmark. The inset illustrates the geometry of the spin systems and the partitioning strategy where we group 8 adjacent qubits as subsystems. (b) The errors for the average magnetisation and correlation using 5×10^5 samples.

the exact simulation of larger quantum systems becomes exponentially costly. To benchmark PQS for larger systems, we investigated a 1D 48-site spin chain with nearest-neighbour correlations, using the time-evolving block decimation (TEBD) method with matrix product states as the reference. As shown in Fig. 2, our simulation results coincide with those of TEBD, which again verifies the reliability of PQS for simulating multiple subsystems. Intriguingly, PQS only needs to manipulate $8+1$ qubits to recover the joint dynamics of the 48-qubits system.

We only consider the time evolution of small and classically simulable quantum systems for benchmarking our method. However, for all the examples considered here, since the simulation cost is independent of the interaction and initial states of the subsystems, PQS also works when tackling a much larger subsystem with more complicated subsystem interactions. In practice, when we increase the subsystem size to around $n = 50$ qubits and consider general strong interactions, PQS could outstrip the capabilities of classical simulation and reliably probe properties of quantum systems with a small-size quantum processor.

In contrast to direct simulation, PQS could also be more robust to noise attributed to the reduction of quantum sources [61]. To verify such an advantage, we experimentally study the dynamical phase transition of an 8-qubit Ising model with nearest-neighbour correlations on IBMQ hardware. By dividing the system into two subsystems, we use a $4+1$-qubit processor to implement our PQS algorithm and compare the results with conventional direct simulation with 8 qubits, as shown in Fig. 3. For a total evolution time $T = 1$, a first-order Trotterisation is used, which has four steps and a negligible Trotter error. Fig. 3(d1,d2) show the magnetisation and Loschmidt amplitude in ferromagnetic phases. The experimental results clearly demonstrates PQS achieves

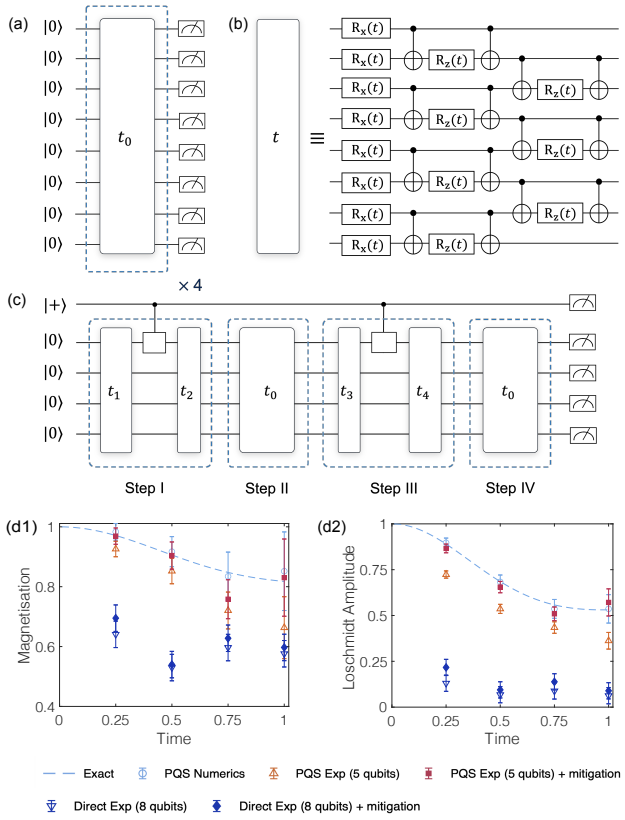

FIG. 3. Implementation and experimental results of the dynamical phase transition of 8 interacting spins. The initial state $|\psi_0\rangle = |0\rangle^{\otimes 8}$ is evolved under 8-site Ising Hamiltonian $H = \sum_j \hat{\sigma}_j^z \hat{\sigma}_{j+1}^z + 0.5 \sum_j \hat{\sigma}_j^x$ with $T = 1$. (a) Quantum circuit for 8-qubit simulation based on first-order Trotterisation with four steps $t_0 = 1/4$. (b) The circuit block for a single-step evolution for time t with parallelisation. (c) An example for the implementation of PQS to simulate 8-qubit system with operations on $4 + 1$-qubit. The circuit blocks are similar as that in (b) with 4 qubits. When a generalised operation is inserted into a Trotter step, we divide the step into two evolution and insert the operation between that. (d) The magnetisation and Loschmidt amplitude in ferromagnetic and paramagnetic phases. Here, the Loschmidt amplitude $\mathcal{G}(t) = \left|\langle\psi_0|e^{-iHt}|\psi_0\rangle\right|^2$ characterises the dynamical echo back to the initial state [60], as an indicator of dynamical phase transition when it decreases to 0. We compare the results of exact simulation (dashed line), PQS (numerics, circle), PQS using IBMQ (5 qubits in (c), upper triangle) and the direct simulation using IBMQ (8 qubits in (a), lower triangle). We also show the results using measurement error mitigation for PQS (solid square) and direct simulation (solid diamond).

higher simulation accuracy than direct simulation. It is also found that with measurement error mitigation, PQS approaches the exact result [62], and outperforms direct simulation consistently. More experimental results and detailed discussions on the implementation and noise robustness of PQS can be found in Sec. VII in [44].

Conclusion and discussion.—Our theoretical, numerical, and experimental results indicate that quantum simulation and perturbation theory are not only compatible but complementary. The PQS algorithm leverages quantum computers to simulate the major component of the Hamiltonian, alleviating the constraint of a classical perturbation method, and uses classical perturbation to approximate the interaction, circumventing limited quantum resources in near-term or early-stage fault-tolerant quantum computers. Since PQS is a hybrid method that combines quantum computing and classical perturbation theory, it inherits their advantages as well as their limitations, such as high-dimensional systems with strong correlations V^{int} and long time T. Yet, PQS is applicable to intermediate-size systems, such as a square lattice with tens to hundreds of qubits, and it is particularly useful for large systems with weak inter-subsystem interactions, such as (quasi) one-dimensional systems and clustered subsystems. Our numerical and experimental results demonstrate wide applicability of PQS methods for studying new physical phenomena, and its potential application in benchmarking large quantum processors with small ones, an emerging demand in the NISQ era. Meanwhile, we could integrate other classical perturbation treatments of the interaction with quantum computing, such as the one that expands according to the interaction strength. We might also consider other hybrid approaches, such as tensor networks, to effectively solve complex many-body systems while alleviating the simulation cost. One may also apply the idea of PQS to more efficiently emulate large quantum circuits using smaller ones [32, 63–67].

Acknowledgments.—J.S. thank Xiao-Ming Zhang and Chenbing Wang for the valuable discussions. X.Y. was supported by Simons Foundation and the National Natural Science Foundation of China Grant No. 12175003. P.H. was supported by AFOSR FA9550-19-1-0369. S.E. is supported by Moonshot R&D, JST, Grant No. JPMJMS2061; MEXT Q-LEAP Grant No. JPMXS0120319794, and PRESTO, JST, Grant No. JPMJPR2114. We acknowledge use of the IBM quantum cloud experience for this work. The views expressed are those of the authors and do not reflect the official policy or position of IBM or the IBMQ team. The numerics are supported by the University of Oxford Advanced Research Computing (ARC) facility and high-performance Computing Platform of Peking University.

* xiaoyuan@pku.edu.cn

[1] I. M. Georgescu, S. Ashhab, and F. Nori, Rev. Mod. Phys. **86**, 153 (2014).
[2] F. Arute, K. Arya, R. Babbush, D. Bacon, J. C. Bardin, R. Barends, R. Biswas, S. Boixo, F. G. Brandao, D. A.

Buell, *et al.*, Nature **574**, 505 (2019).
[3] H.-S. Zhong, H. Wang, Y.-H. Deng, M.-C. Chen, L.-C. Peng, Y.-H. Luo, J. Qin, D. Wu, X. Ding, Y. Hu, P. Hu, X.-Y. Yang, W.-J. Zhang, H. Li, Y. Li, X. Jiang, L. Gan, G. Yang, L. You, Z. Wang, L. Li, N.-L. Liu, C.-Y. Lu, and J.-W. Pan, Science **370**, 1460 (2020).
[4] H.-S. Zhong, Y.-H. Deng, J. Qin, H. Wang, M.-C. Chen, L.-C. Peng, Y.-H. Luo, D. Wu, S.-Q. Gong, H. Su, Y. Hu, P. Hu, X.-Y. Yang, W.-J. Zhang, H. Li, Y. Li, X. Jiang, L. Gan, G. Yang, L. You, Z. Wang, L. Li, N.-L. Liu, J. J. Renema, C.-Y. Lu, and J.-W. Pan, Phys. Rev. Lett. **127**, 180502 (2021).
[5] Y. Wu, W.-S. Bao, S. Cao, F. Chen, M.-C. Chen, X. Chen, T.-H. Chung, H. Deng, Y. Du, D. Fan, M. Gong, C. Guo, C. Guo, S. Guo, L. Han, L. Hong, H.-L. Huang, Y.-H. Huo, L. Li, N. Li, S. Li, Y. Li, F. Liang, C. Lin, J. Lin, H. Qian, D. Qiao, H. Rong, H. Su, L. Sun, L. Wang, S. Wang, D. Wu, Y. Xu, K. Yan, W. Yang, Y. Yang, Y. Ye, J. Yin, C. Ying, J. Yu, C. Zha, C. Zhang, H. Zhang, K. Zhang, Y. Zhang, H. Zhao, Y. Zhao, L. Zhou, Q. Zhu, C.-Y. Lu, C.-Z. Peng, X. Zhu, and J.-W. Pan, Phys. Rev. Lett. **127**, 180501 (2021).
[6] M. Gong, S. Wang, C. Zha, M.-C. Chen, H.-L. Huang, Y. Wu, Q. Zhu, Y. Zhao, S. Li, S. Guo, *et al.*, Science **372**, 948–952 (2021).
[7] X. Mi, P. Roushan, C. Quintana, S. Mandrà, J. Marshall, C. Neill, F. Arute, K. Arya, J. Atalaya, R. Babbush, J. C. Bardin, R. Barends, J. Basso, A. Bengtsson, S. Boixo, A. Bourassa, M. Broughton, B. B. Buckley, D. A. Buell, B. Burkett, N. Bushnell, Z. Chen, B. Chiaro, R. Collins, W. Courtney, S. Demura, A. R. Derk, A. Dunsworth, D. Eppens, C. Erickson, E. Farhi, A. G. Fowler, B. Foxen, C. Gidney, M. Giustina, J. A. Gross, M. P. Harrigan, S. D. Harrington, J. Hilton, A. Ho, S. Hong, T. Huang, W. J. Huggins, L. B. Ioffe, S. V. Isakov, E. Jeffrey, Z. Jiang, C. Jones, D. Kafri, J. Kelly, S. Kim, A. Kitaev, P. V. Klimov, A. N. Korotkov, F. Kostritsa, D. Landhuis, P. Laptev, E. Lucero, O. Martin, J. R. McClean, T. McCourt, M. McEwen, A. Megrant, K. C. Miao, M. Mohseni, S. Montazeri, W. Mruczkiewicz, J. Mutus, O. Naaman, M. Neeley, M. Newman, M. Y. Niu, T. E. O'Brien, A. Opremcak, E. Ostby, B. Pato, A. Petukhov, N. Redd, N. C. Rubin, D. Sank, K. J. Satzinger, V. Shvarts, D. Strain, M. Szalay, M. D. Trevithick, B. Villalonga, T. White, Z. J. Yao, P. Yeh, A. Zalcman, H. Neven, I. Aleiner, K. Kechedzhi, V. Smelyanskiy, and Y. Chen, Science **0**, eabg5029 (2021), https://www.science.org/doi/pdf/10.1126/science.abg5029.
[8] E. T. Campbell, B. M. Terhal, and C. Vuillot, Nature **549**, 172 (2017).
[9] J. Preskill, Quantum **2**, 79 (2018).
[10] S. McArdle, S. Endo, A. Aspuru-Guzik, S. C. Benjamin, and X. Yuan, Rev. Mod. Phys. **92**, 015003 (2020).
[11] M. Cerezo, A. Arrasmith, R. Babbush, S. C. Benjamin, S. Endo, K. Fujii, J. R. McClean, K. Mitarai, X. Yuan, L. Cincio, and et al., Nature Reviews Physics **3**, 625–644 (2021).
[12] K. Bharti, A. Cervera-Lierta, T. H. Kyaw, T. Haug, S. Alperin-Lea, A. Anand, M. Degroote, H. Heimonen, J. S. Kottmann, T. Menke, *et al.*, arXiv preprint arXiv:2101.08448 (2021).
[13] E. Altman, K. R. Brown, G. Carleo, L. D. Carr, E. Demler, C. Chin, B. DeMarco, S. E. Economou, M. A. Eriksson, K.-M. C. Fu, M. Greiner, K. R. Hazzard, R. G. Hulet, A. J. Kollár, B. L. Lev, M. D. Lukin, R. Ma, X. Mi, S. Misra, C. Monroe, K. Murch, Z. Nazario, K.-K. Ni, A. C. Potter, P. Roushan, M. Saffman, M. Schleier-Smith, I. Siddiqi, R. Simmonds, M. Singh, I. Spielman, K. Temme, D. S. Weiss, J. Vučković, V. Vuletić, J. Ye, and M. Zwierlein, PRX Quantum **2**, 017003 (2021).
[14] B. Bauer, S. Bravyi, M. Motta, and G. K.-L. Chan, Chemical Reviews **120**, 12685 (2020).
[15] A. A. Abrikosov, L. P. Gorkov, and I. E. Dzyaloshinski, *Methods of quantum field theory in statistical physics* (Courier Corporation, 2012).
[16] E. Fradkin, *Field theories of condensed matter physics* (Cambridge University Press, 2013).
[17] M. Rigol, T. Bryant, and R. R. Singh, Phys. Rev. E **75**, 061118 (2007).
[18] M. Rigol, T. Bryant, and R. R. Singh, Phys. Rev. Lett. **97**, 187202 (2006).
[19] S. Wilson, Computer Physics Reports **2**, 391 (1985).
[20] G. Rohringer, H. Hafermann, A. Toschi, A. Katanin, A. Antipov, M. Katsnelson, A. Lichtenstein, A. Rubtsov, and K. Held, Rev. Mod. Phys. **90**, 025003 (2018).
[21] G. Knizia and G. K.-L. Chan, Phys. Rev. Lett. **109**, 186404 (2012).
[22] G. Knizia and G. K.-L. Chan, J. Chem. Theory Comput. **9**, 1428 (2013).
[23] S. Wouters, C. A. Jiménez-Hoyos, Q. Sun, and G. K.-L. Chan, J. Chem. Theory Comput. **12**, 2706 (2016).
[24] N. C. Rubin, arXiv preprint arXiv:1610.06910 (2016).
[25] B. Bauer, D. Wecker, A. J. Millis, M. B. Hastings, and M. Troyer, Phys. Rev. X **6**, 031045 (2016).
[26] I. Rungger, N. Fitzpatrick, H. Chen, C. H. Alderete, H. Apel, A. Cowtan, A. Patterson, D. M. Ramo, Y. Zhu, N. H. Nguyen, E. Grant, S. Chretien, L. Wossnig, N. M. Linke, and R. Duncan, arXiv preprint arXiv:1910.04735 (2020).
[27] H. Chen, M. Nusspickel, J. Tilly, and G. H. Booth, Phys. Rev. A **104**, 032405 (2021).
[28] M. Rossmannek, P. K. Barkoutsos, P. J. Ollitrault, and I. Tavernelli, J. Chem. Phys. **154**, 114105 (2021), https://doi.org/10.1063/5.0029536.
[29] H. Ma, M. Govoni, and G. Galli, npj Computational Materials **6**, 85 (2020).
[30] N. Sheng, C. Vorwerk, M. Govoni, and G. Galli, "Quantum simulations of material properties on quantum computers," (2021).
[31] F. Barratt, J. Dborin, M. Bal, V. Stojevic, F. Pollmann, and A. G. Green, npj Quantum Information **7**, 1 (2021).
[32] X. Yuan, J. Sun, J. Liu, Q. Zhao, and Y. Zhou, Phys. Rev. Lett. **127**, 040501 (2021).
[33] A. Eddins, M. Motta, T. P. Gujarati, S. Bravyi, A. Mezzacapo, C. Hadfield, and S. Sheldon, PRX Quantum **3**, 010309 (2022).
[34] P. Huembeli, G. Carleo, and A. Mezzacapo, "Entanglement forging with generative neural network models," (2022), arXiv:2205.00933 [quant-ph].
[35] T. Takeshita, N. C. Rubin, Z. Jiang, E. Lee, R. Babbush, and J. R. McClean, Phys. Rev. X **10**, 011004 (2020).
[36] Z.-X. Li and H. Yao, Annual Review of Condensed Matter Physics **10**, 337 (2019).
[37] W. J. Huggins, B. A. O'Gorman, N. C. Rubin, D. R. Reichman, R. Babbush, and J. Lee, Nature **603**, 416 (2022).
[38] X. Xu and Y. Li, arXiv e-prints , arXiv:2205.14903 (2022), arXiv:2205.14903 [quant-ph].

[39] G. Mazzola and G. Carleo, arXiv e-prints , arXiv:2205.09203 (2022), arXiv:2205.09203 [quant-ph].

[40] T. L. Patti, O. Shehab, K. Najafi, and S. F. Yelin, arXiv e-prints , arXiv:2112.02190 (2021), arXiv:2112.02190 [quant-ph].

[41] Y. Zhang, Y. Huang, J. Sun, D. Lv, and X. Yuan, arXiv e-prints , arXiv:2206.10431 (2022), arXiv:2206.10431 [quant-ph].

[42] The assumptions of the embedding methods and comparisons to our method are discussed in [44].

[43] For instance, the lattice Hamiltonian with multiple degrees of freedom and molecular systems with virtual and active orbitals or in a clustered structure (see Refs. [14, 17, 68] and Sec. V of Supplemental Materials for more discussions) provide a natural partitioning strategy for the subsystems, similarly as that in perturbation theory.

[44] See Supplementary Materials for the framework of generalised quantum operations and perturbative quantum simulation, implementation, resource analysis, derivations and proof, higher-order moment analysis, applications and numerical simulations, experimental demonstrations on IBM quantum devices, which includes Refs. [69–78].

[45] S. Bravyi, M. B. Hastings, and F. Verstraete, Phys. Rev. Lett. **97**, 050401 (2006).

[46] Z. Yan, Y.-R. Zhang, M. Gong, Y. Wu, Y. Zheng, S. Li, C. Wang, F. Liang, J. Lin, Y. Xu, *et al.*, Science **364**, 753 (2019).

[47] Y. Lahini, M. Verbin, S. D. Huber, Y. Bromberg, R. Pugatch, and Y. Silberberg, Phys. Rev. A **86**, 011603 (2012).

[48] M. A. Cazalilla, R. Citro, T. Giamarchi, E. Orignac, and M. Rigol, Rev. Mod. Phys. **83**, 1405 (2011).

[49] F. Arute, K. Arya, R. Babbush, D. Bacon, J. C. Bardin, R. Barends, A. Bengtsson, S. Boixo, M. Broughton, B. B. Buckley, *et al.*, arXiv preprint arXiv:2010.07965 (2020).

[50] I. D. Kivlichan, J. McClean, N. Wiebe, C. Gidney, A. Aspuru-Guzik, G. K.-L. Chan, and R. Babbush, Phys. Rev. Lett. **120**, 110501 (2018).

[51] Z. Jiang, K. J. Sung, K. Kechedzhi, V. N. Smelyanskiy, and S. Boixo, Phys. Rev. Appl. **9**, 044036 (2018).

[52] P. Jurcevic, B. P. Lanyon, P. Hauke, C. Hempel, P. Zoller, R. Blatt, and C. F. Roos, Nature **511**, 202 (2014).

[53] C. Monroe, W. Campbell, L.-M. Duan, Z.-X. Gong, A. Gorshkov, P. Hess, R. Islam, K. Kim, N. Linke, G. Pagano, *et al.*, Rev. Mod. Phys. **93**, 025001 (2021).

[54] A. M. Childs, D. Maslov, Y. Nam, N. J. Ross, and Y. Su, Proceedings of the National Academy of Sciences **115**, 9456 (2018).

[55] A. M. Childs, Y. Su, M. C. Tran, N. Wiebe, and S. Zhu, Phys. Rev. X **11**, 011020 (2021).

[56] G. H. Low and I. L. Chuang, Quantum **3**, 163 (2019).

[57] G. H. Low and I. L. Chuang, Phys. Rev. Lett. **118**, 010501 (2017).

[58] We discuss the implementation with a truncated expansion on a quantum computer in Sec. III in [44].

[59] For example, the condition holds when $V^{\mathrm{int}} = \lambda_1 X_a Y_b Z_c + \lambda_2 Y_a Z_b X_c + \lambda_3 Z_a X_b Y_c$ with Pauli operators X, Y, and Z acting on three subsystems a, b, and c. To have a reasonable overhead C, the algorithm is efficient when $\lambda_T = \sum_i |\lambda_i| T$, aligning with the spirit of perturbation theory.

[60] P. Jurcevic, H. Shen, P. Hauke, C. Maier, T. Brydges, C. Hempel, B. P. Lanyon, M. Heyl, R. Blatt, and C. F. Roos, Phys. Rev. Lett. **119**, 080501 (2017).

[61] A smaller quantum device is usually much more accurate than a larger quantum processor due to crosstalks or other types of errors when controlling large quantum systems. Our method could thus serve as a benchmark of the computing result for large-scale problems.

[62] S. Bravyi, S. Sheldon, A. Kandala, D. C. Mckay, and J. M. Gambetta, Phys. Rev. A **103**, 042605 (2021).

[63] T. Peng, A. W. Harrow, M. Ozols, and X. Wu, Phys. Rev. Lett. **125**, 150504 (2020).

[64] F. Barratt, J. Dborin, M. Bal, V. Stojevic, F. Pollmann, and A. G. Green, npj Quantum Information **7** (2021), 10.1038/s41534-021-00420-3.

[65] K. Mitarai and K. Fujii, New Journal of Physics **23**, 023021 (2021).

[66] K. Fujii, K. Mitarai, W. Mizukami, and Y. O. Nakagawa, arXiv e-prints , arXiv:2007.10917 (2020), arXiv:2007.10917 [quant-ph].

[67] K. Mitarai and K. Fujii, Quantum **5**, 388 (2021).

[68] E. Garlatti, T. Guidi, S. Ansbro, P. Santini, G. Amoretti, J. Ollivier, H. Mutka, G. Timco, I. Vitorica-Yrezabal, G. Whitehead, *et al.*, Nature communications **8**, 1 (2017).

[69] D. Greenbaum, arXiv preprint arXiv:1509.02921 (2015).

[70] G. Aleksandrowicz, T. Alexander, P. Barkoutsos, L. Bello, Y. Ben-Haim, *et al.*, "Qiskit: An Open-source Framework for Quantum Computing," (2019).

[71] S. Endo, S. C. Benjamin, and Y. Li, Phys. Rev. X **8**, 031027 (2018).

[72] J. Sun, X. Yuan, T. Tsunoda, V. Vedral, S. C. Benjamin, and S. Endo, Phys. Rev. Appl. **15**, 034026 (2021).

[73] M. Kieferová, A. Scherer, and D. W. Berry, Phys. Rev. A **99**, 042314 (2019).

[74] Y.-H. Chen, A. Kalev, and I. Hen, arXiv preprint arXiv:2103.15334 (2021).

[75] I. H. Kim, arXiv preprint arXiv:1702.02093 (2017).

[76] J. Šmakov, A. Chernyshev, and S. R. White, Phys. Rev. Lett. **98**, 266401 (2007).

[77] K. Xu, Z.-H. Sun, W. Liu, Y.-R. Zhang, H. Li, H. Dong, W. Ren, P. Zhang, F. Nori, D. Zheng, *et al.*, Science advances **6**, eaba4935 (2020).

[78] J. Zhang, G. Pagano, P. W. Hess, A. Kyprianidis, P. Becker, H. Kaplan, A. V. Gorshkov, Z.-X. Gong, and C. Monroe, Nature **551**, 601 (2017).